EPJ Web of Conferences **119**, 13001 (2016) DOI: 10.1051/epjconf/201611913001
ILRC 27

LIDAR SOUNDINGS BETWEEN 30 AND 100 KM ALTITUDE DURING DAY AND NIGHT FOR OBSERVATION OF TEMPERATURES, GRAVITY WAVES AND TIDES

Michael Gerding*, Kathrin Baumgarten, Josef Höffner, Franz-Josef Lübken

Leibniz-Institute of Atmospheric Physics at the Rostock University, Kühlungsborn, Germany
**Email: gerding@iap-kborn.de*

ABSTRACT

Ground-based temperature measurements by lidar are an important tool for the understanding of long-term temperature changes as well as the propagation of gravity waves and tides. Though, mesospheric soundings are often limited to nighttime conditions due to the low signal-to-noise ratio during the day. We developed a daylight-capable RMR lidar for temperature soundings in the middle atmosphere. The influences of the narrowband detector on the calculated hydrostatic temperatures as well as their correction are described. The RMR lidar is complemented by a co-located resonance lidar. We present an example for tidal analyses and short-term variability of tidal amplitudes.

1. INTRODUCTION

Temperature is one of the key parameters needed for the understanding of dynamical and chemical processes in the whole atmosphere. Lidar is the only ground-based technique providing continuous temperature profiles from the troposphere up to the lower thermosphere (e.g. [1]). Depending on altitude, rotational and vibrational Raman scattering, Rayleigh and/or resonance scattering are used. Long-term data sets of precise lidar-derived temperature profiles are important for the understanding of climate change in the whole middle atmosphere [2]. Temporally resolved temperature data can be used to derive (altitude resolved) amplitudes of gravity waves, tidal and planetary waves (e.g. [3]). Unfortunately, especially Rayleigh lidars are often limited to nighttime conditions, as the solar background radiation typically exceeds the laser backscatter from the mesosphere by several orders of magnitude. By this, observations of tides and planetary waves are inhibited. Observations of absolute temperatures and trends are restricted to nighttime only, impeding comparisons with other data sets.

In 2010 we developed a new RMR lidar at our site at Kühlungsborn/Germany (54°N, 12°E), subsequently replacing an old RMR lidar observing middle atmospheric temperatures since 2002 [1,4]. The old lidar is lacking effective daylight suppression and was operated during nighttime only. The new RMR lidar is designed for observations of noctilucent clouds at 532 nm [5] and for measurements of temperature profiles up to ~75 km (~90 km) during day (night), respectively. Until autumn 2012 the lidar has been complemented by a daylight-capable potassium resonance lidar for temperature observations between ~85 and 105 km. The old RMR lidar was operated in parallel during nighttime until August 2013.

A first study of tidal temperature variations has been published by [6]. Here we provide an overview of the instrumental setup and the correction of filter effects (Section 2). In Section 3 we show an example of tidal temperature variations.

2. METHODOLOGY

The new RMR lidar is based on an injection-seeded Nd:YAG laser used at second harmonic (532 nm). The external seedlaser is locked to an iodine absorption line. Detailed information is given in Table 1. The laser is emitted co-axially with the receiving telescope by means of different steerable mirrors. A beam-stabilization based on a Piezo-coupled mirror is used to keep the laser beam within the 62 μrad field of view of the telescope [7]. Input for beam-stabilization is provided by a CCD camera observing the beam in real-time through the same telescope and a 90:10 beam splitter. The received signal is guided to a detection bench consisting essentially of a narrow-band optical filter (interference filter and double-etalon) and an avalanche photodiode.

Table 1: Summary of instrument parameters of the new RMR lidar at Kühlungsborn

wavelength (vac.) [nm]	532.24
power @ 532 nm [W]	~ 22
repetition rate [pps]	30
beam diameter after expansion [m]	0.09
beam divergence after expansion [μrad]	50
field of view [μrad]	62
telescope diameter [m]	0.81
interference filter width (FWHM) [pm]	130
etalon 1 free spectral range [pm]	120
etalon 1 observed finesse	27
etalon 2 free spectral range [pm]	140
etalon 2 observed finesse	20

The bandwidth of the etalons is only about 4 pm, i.e. comparable to the Doppler-broadened Rayleigh backscatter (~2.5 pm). Due to the Airy shape of the transmission functions of both etalons, part of the Rayleigh backscatter is suppressed by the etalons. The overall transmission is reduced to 80 – 90% of the transmission of the unbroadened light. Figure 1 shows the transmission function of the first etalon and the spectrum of the Doppler-broadened backscatter before and after the etalon.

Obviously, the transmission of the etalon depends on the atmospheric temperature at the particular

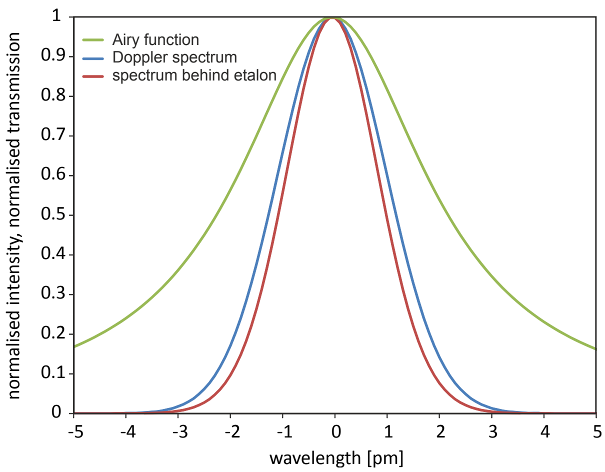

Fig. 1: Transmission of first etalon and relative intensity. Doppler broadening calculated for 300 K.

scattering altitude. By this, an altitude dependent factor must be added to the lidar equation. This factor needs to be accounted for calculation of a relative density profile from the photon count profile. The relative density profile is a pre-requisite for temperature inversion [8]. We have implemented an iterative transmission correction to get the correct density profile. The algorithm first calculates temperatures ignoring the transmission effect. Based on this temperature profile the nominal transmission is retrieved and used for correction of the photon count profile. The corrected backscatter profile is again inverted into temperatures. Figure 2 shows the temperature profiles with and without transmission correction in comparison with the data of the old RMR lidar being operated simultaneously. Please note that both lidars are completely independent systems, using different lasers, telescopes, detectors etc. Above the Rayleigh temperature profile we show the K lidar data that is used for seeding the inversion of the data from the old lidar. Below 43 km no correction is necessary for the new RMR lidar, because in this range a separate detector in front of the double etalon is used. The systematic error of the uncorrected profile increases from 85 km down to ~60 km due to increasing temperature, i.e. decreasing transmission of the etalons. Below 60 km the effect is reverse due to the changing temperature

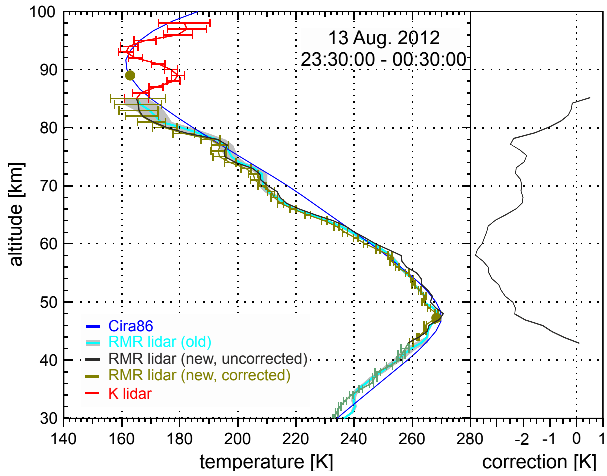

Fig. 2: Temperature profile of 14 August 2008, 0 UT obtained by old and new RMR lidar, and K lidar. The right profile shows the difference between uncorrected and true Rayleigh temperature profile.

gradient. The differences between temperatures of both RMR lidars are within the statistical uncertainty after correction. The inversion of the new lidar data is independently seeded by CIRA-86 temperatures [9] at 89 km.

We do not show data below 30 km altitude due to the increasing effect of aerosols. An aerosol correction is currently under development.

3. RESULTS

Between June 2010 and December 2014 the new RMR lidar was in operation for ~5200 hours. Soundings continue since whenever weather allows. Figure 3 shows a sounding running for ~16 h during 13/14 August 2012 (cf. profile presented in Fig. 2). Temperatures are calculated with a running average of 2 h. The solar elevation during the sounding was up to 50°. Please note that local solar time (LST) at Kühlungsborn is ~45 min ahead of UT. During the day the uppermost altitude for RMR temperature retrieval decreases due to increasing noise. Simultaneously the available height range from the K lidar shrinks. During the night (until ~4 UT) the gap at 80 km occurs due to the use of CIRA-86 instead of K lidar data for Rayleigh temperature retrieval. Fig. 3 shows some temporal variation of temperatures due to gravity waves and tides.

For a quantitative analysis of wave amplitudes the deviations of temperatures from the daily mean profile are examined. As described by [6], typically ~100 h of lidar data are used to calculate amplitudes and phases of 24 h, 12 h, and 8 h waves for each available altitude bin. Depending on weather conditions, each harmonic fit covers a period of ~4 – 30 d. Variability of tidal amplitudes can be large in the middle atmosphere due to changing transmission conditions for the particular wave modes. Figure 4 shows tidal amplitudes for different periods in September 2014 together with the monthly mean. Here only the diurnal and semidiurnal variations are considered due to possible confusion of the terdiurnal tide and long-period gravity waves on short time scales. Mean amplitudes of the 24 h tide are around 1 K up to 65 km and partly up to 2 K between 45 and 50 km. Above 65 km the amplitude increases strongly. The semidiurnal tide is somewhat smaller in the stratopause region (0.5 – 1 K), increasing steadily above 55 km.

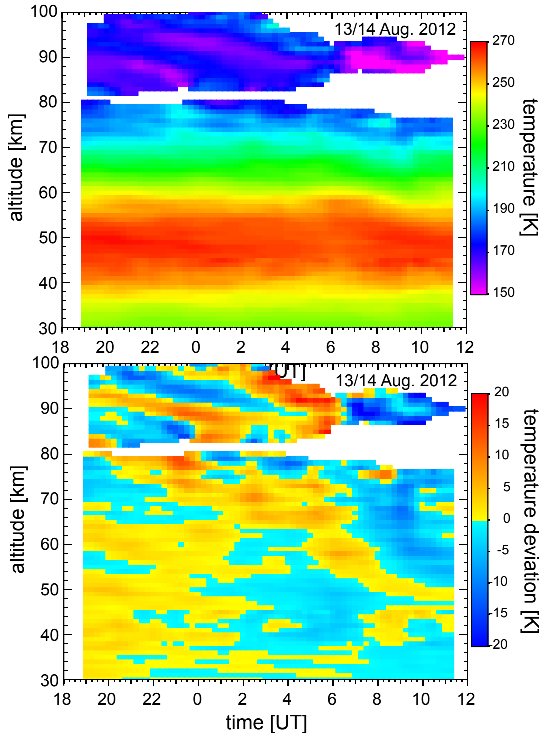

Figure 3: Temporal variation of temperatures during night and day. Solar elevation was up to 50°. Upper plot: absolute temperatures, lower plot: deviation from the daily mean profile.

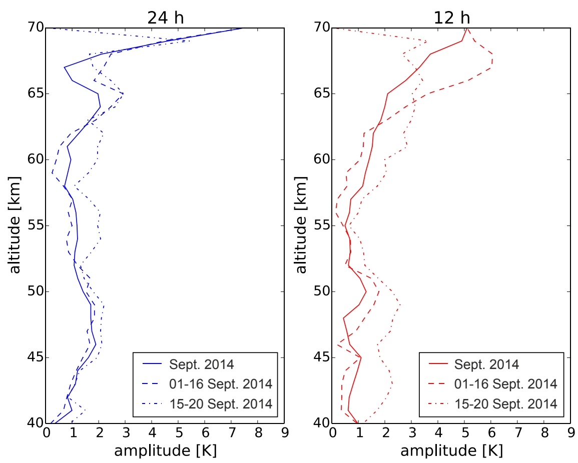

Figure 4: Amplitudes of diurnal and semidiurnal variations for different periods in September 2014 (period 1: 96 h, period 2: 101 h) and for the monthly mean.

Depending on altitude, amplitudes in the shorter sounding periods often vary by 100% or even more. The monthly mean amplitude in some altitudes ranges is smaller than the average of the individual periods, e.g. around 50 km and 65 km for both harmonics. This indicates a phase shift of the tide between both sounding periods due to, e.g., changing propagation conditions. Further analysis of the propagation conditions of individual tidal modes is outside the scope of this paper.

4. CONCLUSIONS

We have shown that effective daylight suppression by means of a narrow field of view and narrowband optical filters allows Rayleigh temperature soundings in the middle atmosphere up to ~75 km during the day. We perform regular RMR lidar temperature soundings during day and night at Kühlungsborn/Germany since 2010, complemented until autumn 2012 by a K resonance lidar. The transmission of the etalons depends on the Doppler broadening of the backscatter signal. This temperature (or altitude) dependent effect results in a systematic temperature bias of up to ~4 K. We correct the backscatter profile in an iterative process making use of an initially calculated temperature profile. The final temperature profile agrees well with the simultaneous, co-located data of the old RMR lidar. Continuous lidar soundings allow the calculation of tidal amplitudes and phases. While many other instruments like space-based profilers require about 2 months for tide observations, lidar requires only about 4 days of sounding, if weather allows. Tidal variability can be at least 100% in amplitude, if short-term data are compared with, e.g., a monthly average. Altitude ranges where the average amplitude is lower than short-term data indicate a change in phase progression, e.g., due to changing propagation conditions. Future soundings will allow further studies of tidal variability above our mid-latitude station, as well as the separation of gravity waves and tides.

ACKNOWLEDGEMENT

The authors gratefully acknowledge Maren Kopp for her help in the installation of the new RMR lidar. We thank Torsten Köpnick and Michael Priester for the maintenance and operation of the lidar systems at IAP. We also acknowledge all our students for their numerous hours of lidar operation. This research has been partly supported by the Deutsche Forschungsgemeinschaft (DFG) under Grant GE 1625/2-1.

REFERENCES

[1] Alpers, M., R. Eixmann, C. Fricke-Begemann, M. Gerding, and J. Höffner, 2004: Temperature lidar measurements from 1 to 105 km altitude using resonance, Rayleigh, and Rotational Raman scattering, *Atmos. Chem. Phys.*, ***4*,** 793-800

[2] Angot, G., P. Keckhut, A. Hauchecorne, and C. Claud, 2012: Contribution of stratospheric warmings to temperature trends in the middle atmosphere from the lidar series obtained at Haute-Provence Observatory (44°N), *J. Geophys. Res.*, **117,** D21102, doi: 10.1029/2012JD017631

[3] Gerrard, A. J., Y. Bhattacharya, and J. P. Thayer, 2011, Observations of in-situ generated gravity waves during a stratospheric temperature enhancement (STE) event, *Atmos. Chem. Phys.,* **11**, 11913–11917

[4] Gerding, M., J. Höffner, J. Lautenbach, M. Rauthe, and F.-J. Lübken, 2008: Seasonal variation of temperatures between 1 and 105 km altitude at 54°N observed by lidar, *Atmos. Chem. Phys.*, **8**, 7465-7482

[5] Gerding, M., M. Kopp, P. Hoffmann, J. Höffner, and F.-J. Lübken, 2013: Diurnal variation of mid-latitude NLC parameters observed by daylight-capable lidar and their relation to ambient parameters, *Geophys. Res. Lett.,* **40***,* 6390-6394

[6] Kopp, M., M. Gerding, J. Höffner, and F.-J. Lübken, 2015: Tidal signatures in temperatures derived from daylight lidar soundings above Kühlungsborn (54°N, 12°E), *J. Atmos. Solar-Terr. Phys.*, *127*, 37-50, doi:10.1016/j.jastp.2014.09.002

[7] Eixmann, R., M. Gerding, J. Höffner, and M. Kopp, 2015: Lidars with narrow FOV for spectral and daylight measurements, *IEEE Transactions on Geoscience and Remote Sensing*, in print

[8] Hauchecorne, A., and M.-L. Chanin, 1980: Density and temperature profiles obtained by lidar between 35 and 70 km, *Geophys. Res. Lett.*, **7**, 565–568

[9] Fleming, E. L., S. Chandra, J. J. Barnett, and M. Corney, 1990: Zonal mean temperature, pressure, zonal wind, and geopotential height as functions of latitude, *Adv. Space Res.*, **10**, 11–59